Science of the Total Environment 785 (2021) 147303

Contents lists available at ScienceDirect

Science of the Total Environment

journal homepage: www.elsevier.com/locate/scitotenv

Seasonal discrepancies in peroxyacetyl nitrate (PAN) and its correlation with ozone and $PM_{2.5}$: Effects of regional transport from circumjacent industrial cities

Mei Sun [a], Ying Zhou [a,*], Yifei Wang [a], Xiaochen Zheng [b], Jia'nan Cui [a], Dong Zhang [c], Jianbo Zhang [a,*], Ruiqin Zhang [c]

[a] State Key Joint Laboratory of Environmental Simulation and Pollution Control, College of Environmental Sciences and Engineering, Peking University, Beijing 100871, China
[b] Institute of Environmental Engineering (IfU), ETH Zürich, 8093 Zürich, Switzerland
[c] Research Institute of Environmental Science, College of Chemistry and Molecular Engineering, Zhengzhou University, Zhengzhou 450001, China

HIGHLIGHTS

- Inflow from circumjacent industrial cities ruled the elevated PAN level in winter.
- Joint transport of O_3 or $PM_{2.5}$ with PAN promotes a positive correlation in winter.
- The feature of air masses affects the consistent trend between PAN and O_3.

GRAPHICAL ABSTRACT

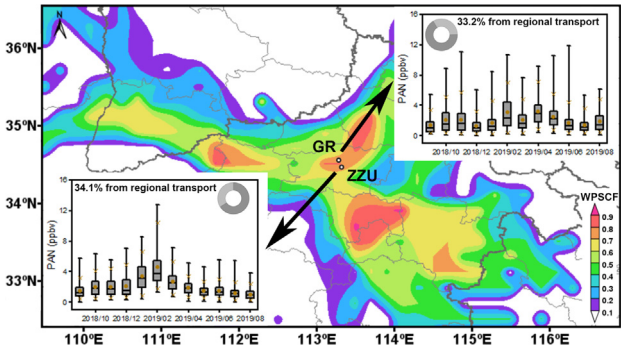

ARTICLE INFO

Article history:
Received 23 November 2020
Received in revised form 16 April 2021
Accepted 18 April 2021
Available online 24 April 2021

Editor: Jianmin Chen

Keywords:
Peroxyacetyl nitrate
Ozone
Fine particulate matter
Regional transport
Industrial urban agglomeration

ABSTRACT

Peroxyacetyl nitrate (PAN) is the most important reservoir of nitrogen oxides, with effects on atmospheric oxidation capacity and regional nitrogen distribution. The first yearlong observational study of PAN was conducted from September 2018 to August 2019 at a suburban site and an urban site in Zhengzhou, Henan Province, central China. Compared with studies over the past two decades, summer PAN pollution at the suburban site and winter PAN pollution at both sites were more significant, with annual average concentrations of 1.96 ± 1.44 and 2.01 ± 1.59 ppbv, respectively. Seasonal PAN discrepancies between the urban and suburban areas were analyzed in detail. Active PAN formation, regional transport, photochemical precursors, and PAN lifetime played key roles during seasons with elevated PAN (winter and spring). According to the results of cluster analysis and potential source contribution function analysis, during the cold months, short-distance air mass transport from the east, south, and southeast of Henan Province and southern Hebei Province increased PAN pollution in urban Zhengzhou. PAN source areas were located in circumjacent industrial cities surrounding Zhengzhou except in the northeastern direction. Based on the relationships between pollutant concentrations, wind speed, and wind direction, a strong positive correlation between PAN and $PM_{2.5}$ (and O_3) existed in winter due to their joint transport. A slow-moving, low-height air mass passed through surrounding industrial cities before reaching the study area, carrying both pollutants and leading to strong consistency between PAN and O_3 levels. The long-term PAN

* Corresponding authors at: State Key Joint Laboratory of Environmental Simulation and Pollution Control, College of Environmental Sciences and Engineering, Peking University, Beijing 100871, China.
E-mail addresses: flora.chow@pku.edu.cn (Y. Zhou), jbzhang@pku.edu.cn (J. Zhang).

https://doi.org/10.1016/j.scitotenv.2021.147303

characteristics described in this study will help clarify the causes of regional air pollution in inland city agglomerations. Moreover, the PAN correlations and joint transport of PAN and $PM_{2.5}$ (or O_3) support the use of PAN as an indicator of air pollution introduced from surrounding industrial areas.

1. Introduction

In recent years, industrial emissions, traffic, and other factors such as meteorological conditions have made air pollution an increasingly prominent problem in China (An et al., 2019; Zhao et al., 2020). Nitrogen oxides (NO_X = nitric oxide [NO] + nitrogen dioxide [NO_2]) and nitrogen reservoir species are closely associated with severe ozone (O_3) and haze pollution (Fischer et al., 2014; Wei et al., 2020). Peroxyacetyl nitrate (PAN; $CH_3COO(O)NO_2$) is the most important atmospheric NO_X reservoir (Roberts, 2007; Payne et al., 2017). PAN forms through secondary reactions involving volatile organic compounds (VOCs) and atmospheric oxidants such as hydroxyl radicals (OH) in the presence of NO_2 (Stephens, 1969; LaFranchi et al., 2009; Xue et al., 2014). As PAN plays a role in the conversion of NO and NO_2, obtaining its temporal variations is crucial to evaluating the budgets of O_3, RO_X, and HO_X (Khan et al., 2017; Crowley et al., 2018). At the regional scale, PAN is sufficiently stable for transport over long distances in cold conditions and thermally decomposes to release NO_2 when the air mass warms (Dassau et al., 2004; Kotchenruther et al., 2001). Hence, the transport of PAN is a potential pathway through which NO_X can reach the regions surrounding a city, impacting the atmospheric oxidation capacity and nitrogen distribution.

Air pollution in China exhibits distinct regional characteristics (Wang and Hao, 2012). Due to the importance of PAN in atmospheric chemistry as described above, thorough analysis of PAN levels and transport can help with identifying the formation mechanisms of severe regional air pollution. Previous research has emphasized that the analysis of pollutant transport should consider the seasonal cycle and related meteorological factors (Wang et al., 2016). However, most PAN related studies have been implemented over short time scales, and thus its activity in the atmosphere over urban agglomerations might have been underestimated. The seasonal variability of PAN was investigated in two coastal cities in southern China (Hu et al., 2020; Wang et al., 2015). The result showed that elevated PAN levels were generally observed when the air masses pass through highly industrialized cities, despite the influence of air masses from both the continent and ocean. Compared with coastal city clusters, which experience cleaning effects from oceanic air masses, inland urban agglomerations with intensive industrial activities are significantly more strongly affected by air masses carrying pollution from production activities and traffic emissions throughout the year (Li et al., 2021; Xiao et al., 2017; Yang et al., 2020). Consequently, compared with the reports from coastal city clusters, PAN transport in inland areas may exhibit different trends reflective of greater impacts due to the mobility of air masses among cities. To the best of our knowledge, no reference data yet exist for long-term PAN levels in inland urban agglomerations, except for Beijing and the surrounding areas (Beijing-Tianjin-Hebei [BTH] region) (G. Zhang et al., 2014; Wei et al., 2020; Qiu et al., 2020). This lack of relevant research hinders the full elucidation of regional air pollution.

The atmospheric activity of PAN is closely related to the severity of O_3 or aerosol pollution (G. Zhang et al., 2014). PAN and tropospheric O_3 are produced through photochemical reactions and associated with negative impacts on vegetation and human health (Vyskocil et al., 1998; Lefohn et al., 2018). Both constituents form through processes that occur at the local and regional scales (Malley et al., 2016). Previously, researchers have attempted to characterize the decoupling between PAN and O_3, which usually results from low photochemical intensity (Zhang et al., 2019), different removal pathways (Zhang et al., 2020), or air mass transport (Malley et al., 2016; Han et al., 2017). In comparison, good consistency between PAN and O_3 has mainly been considered to result from intensive photochemical activity at the local scale. Nevertheless, little research has investigated the effects of regional transport on the strength of the correlation between the two pollutants. Recently, coinciding increases and decreases of PAN and O_3 were attributed to air masses arriving from continental and oceanic sources by Hu et al. (2020). However, transport effects remain unclear due to the lack of data representing inland regions, especially for inter-city transport. In addition, researchers are paying increasing attention to the relationship between PAN and particulate matter with an aerodynamic diameter of less than 2.5 μm ($PM_{2.5}$), which reflects the history of the air mass and degree of photochemical aging (Wolfe et al., 2007). Han et al. (2017) reported that the transport of aerosol pollution across continents could be tracked by investigating the relationship between PAN and $PM_{2.5}$ (and its composition). According to a study conducted in Beijing, concentrations of both PAN and $PM_{2.5}$ related to regional transport accounted for significant proportions of the total levels during a haze pollution period (Qiu et al., 2019b). However, the correlation between PAN and $PM_{2.5}$ is not well characterized in terms of regional or inter-city pollution transport. Therefore, determining the impacts of air mass transport on the relationships of PAN with O_3 and $PM_{2.5}$ in inland urban agglomerations is essential and will support the development of effective joint control strategies.

Here, we conducted simultaneous 1-year field observations at an urban site and a suburban site in Zhengzhou, a core city in the industry-intensive inland urban agglomeration of central China. The objectives of this study were to identify and characterize the temporal and spatial discrepancies in PAN under different atmospheric conditions caused by seasonal variations, determine the local and distant contributions to PAN, identify the potential source regions of transported PAN, and elucidate the mechanism through which wind conditions and air mass transport affect the relationships of PAN with O_3 and $PM_{2.5}$. This study would improve our understanding of regional air pollution in large inland urban agglomerations and provide a basis for using PAN correlations to indicate air pollution events caused by air mass transport.

2. Methodology

2.1. Site description

Zhengzhou, the capital city of Henan Province, is the core city of the Central Plains Economic Region (CPER) and a major industrial city in central China. The secondary industrial output of Zhengzhou accounted for a large proportion (43.9%) of the national industrial output in 2018 (CSY, 2019) relative to other megacities. The rapid development of industrial activities has contributed to serious air pollution in Zhengzhou. In 2018 and 2019, Zhengzhou was one of the 20 cities with the worst air quality in China (https://www.mee.gov.cn/hjzl/sthjzk/). With a population of more than 10 million, improvement of the air quality in Zhengzhou, which would reduce the health risks associated with exposure to high air pollutant concentrations, is urgently needed. Furthermore, Zhengzhou is surrounded by several industrial cities, including Jiaozuo, Luoyang, Pingdingshan, and Xuchang, causing Zhengzhou to be not only a source of pollutants but also a receptor via inter-city transport. Thus, Zhengzhou is an ideal site for studying inter-city PAN transport and the impact of regional air pollution on the relationships of PAN with other species.

Fig. 1 shows the locations of the observation sites in Zhengzhou. The urban site (ZZU; 34°48′47″N, 113°32′20″E) was located on the roof of a building at Zhengzhou University (approximately 20 m above the ground level). The urban site was surrounded by university facilities, residential buildings, and arterial roads. The suburban site was

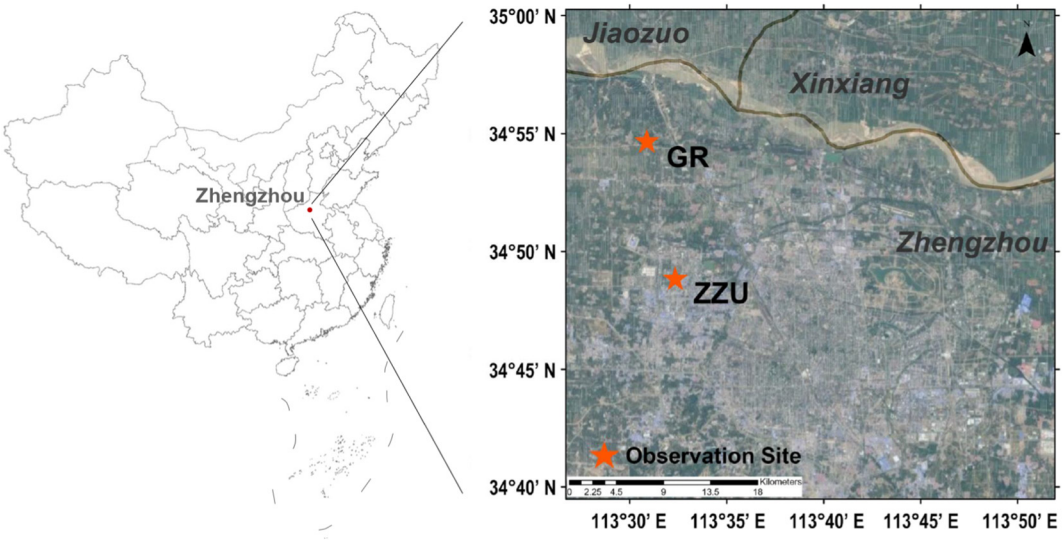

Fig. 1. Location of the observation sites in Zhengzhou.

established at Gangli Reservoir (GR; 34°54′42″N, 113°30′31″E), a National Ambient Air Automatic Monitoring Station (background site) that is located 12 km northwest of the ZZU site. The surrounding environment contains plants, farmland, and sparsely populated low-rise residential apartments. Except for a highway located 400 m to the south, no major air pollution sources were present near the GR site.

2.2. Measurement instruments

Online PAN detectors developed by Peking University were used for PAN measurement at the two sites. Our previous studies have described the structure of the PAN monitoring system in detail (Zhang et al., 2019; Zhu et al., 2018). The measurement and calibration processes are summarized in Supporting Information S1. The PAN analyzer has a temporal resolution of 5 min and a detection limit of 5 pptv. We conducted weekly single-point calibration and monthly multi-point calibration of the PAN instruments in this study to ensure data quality. A calibration standard curve ($R^2 > 0.997$) was obtained for calculating PAN concentrations. The slopes of the fitted lines before and after calibration sometimes exhibited small differences of less than 10%.

During the observation period, the concentrations of O_3, NO_X, sulfur dioxide (SO_2), carbon monoxide (CO), and $PM_{2.5}$ at the ZZU site were continuously measured using appropriate instruments (TE Model 49i, TE Model 42i, TE Model 43i, TE Model 48i, and TEOM 1400a) purchased from Thermo Fisher Scientific (Waltham, MA, USA). Meteorological data, including those for temperature (Temp), relative humidity (RH), barometric pressure (BP), wind speed (WS), wind direction (WD), and precipitation (PRCP), were collected using an automatic weather station (Model QXZ 1.0; Yigu Technology Inc., Wuhan, China) (Wang et al., 2019). The photolysis frequency (j-value) of trace gases was measured using a spectrometer equipped with a cooled charge-coupled device detector purchased from Focused Photonics (Hangzhou, China). The detection limits of the measured species, instrument specifications, and related parameters are listed in Table S1. Pollutant concentrations at the GR site and meteorological data (Temp, RH, BP, WS, WD, and PRCP) were obtained from the Zhengzhou Environmental Protection Monitoring Center Station (http://www.mee.gov.cn).

3. Results and discussion

3.1. Overview of atmospheric PAN levels

In this study, the measured 5-min PAN data were processed into hourly average data for analysis, and a statistical summary is provided in Table 1. During the 1-year observation period, the average PAN concentration at the ZZU site was 1.96 ± 1.44 ppbv (N = 7908), and the maximum value was 12.81 ppbv. The average (2.01 ± 1.59 ppbv) and median concentrations at the GR site (N = 6093) were similar to those at the ZZU site, and the maximum value (11.88 ppbv) was slightly lower than that at the ZZU site. To prevent phytotoxicity and potential biological effects from PAN (Moravek et al., 2015; Taylor, 1969; DeMarini et al., 2000; Lin et al., 2000; Vyskocil et al., 1998), the World Health Organization (WHO) recommends that the 8-h average concentration of PAN should not exceed 5 ppbv (WHO, 1987). In this study, according to the WHO recommendation, any day with a daily maximum 8-h average concentration above 5 ppbv is referred to as an over-limit

Table 1
Statistical summary of PAN concentrations and over-limit days.

Site	Season	Mean PAN concentration (ppbv)	Median PAN concentration (ppbv)	SD (ppbv)	Maximum PAN concentration (ppbv)	Maximum 8-h average PAN concentration (ppbv)	Number of over-limit days
ZZU	Autumn	1.83	1.55	1.13	6.33	5.46	2
	Winter	3.04	2.59	2.06	12.81	12.34	21
	Spring	1.92	1.71	1.05	7.11	5.91	3
	Summer	1.24	1.12	0.77	5.55	3.94	0
	All	1.96	1.55	1.44	12.81	12.34	26
GR	Autumn	1.86	1.37	1.54	11.09	8.41	7
	Winter	1.77	1.24	1.63	10.69	10.12	9
	Spring	2.56	2.20	1.66	10.59	8.92	18
	Summer	1.67	1.29	1.25	11.88	6.3	2
	All	2.01	1.54	1.59	11.88	10.12	36

day. The number of over-limit days was higher at the GR site (36 days) than at the ZZU site (26 days). Most over-limit days occurred in winter at the ZZU site (80.8%), whereas unacceptable PAN levels at the GR site were most frequently recorded in spring (18 days).

We compared the annual and seasonal concentration trends of PAN at the urban and suburban sites in this study with data from previous research (see Tables 1 and S2). The average annual pollution levels of PAN in urban and suburban Zhengzhou were 2.5–3.7 times higher than those in other regions where long-term studies had been conducted (Lee et al., 2013; Wang et al., 2015; Hu et al., 2020). The results of this study were compared with those of long-term or seasonal PAN observational studies in the North China Plain (NCP). The monthly variation pattern differed between urban Zhengzhou and Beijing. The atmospheric level of PAN over Beijing was relatively low (0.28–0.73 ppbv from October to March and 1.37–3.79 ppbv from March to August; G. Zhang et al., 2014). Although the annual average value was higher in suburban Zhengzhou than at a regional background site near Beijing (0.94 ppbv; Qiu et al., 2020), the monthly average values for January (1.70 ppbv), April (3.22 ppbv), July (1.41 ppbv), and October (2.06 ppbv) in this study were lower than the values reported by Wei et al. (2020) for the border of the BTH region.

In summer, the PAN pollution level in the Zhengzhou urban area was lower than most published short-term observations (average concentrations of 1.41–3.79 ppbv; Zhang et al., 2011; Xu et al., 2011; Zhang et al., 2015; Liu et al., 2018; Sun et al., 2020) and higher than the atmospheric level during the period of the Beijing Olympic Games (0.74 ppbv; Gao et al., 2014). In contrast to urban Zhengzhou, the summer PAN level in suburban Zhengzhou was higher than observations from short-term field campaigns in the suburbs of Chongqing (0.84 ppbv; Sun et al., 2020), Lanzhou (0.76 ppbv; Zhang et al., 2009), and Guangzhou (1.32 and 0.507 ppbv; Wang et al., 2010; Yuan et al., 2018) in China. Significantly, the concentrations of PAN in winter measured in this study were higher than the levels reported in all previous short-term studies in China, including both urban and suburban areas (0.31–1.89 ppbv for urban areas and 0.55–1.04 ppbv for suburban areas; Wang et al., 2017; Zhang et al., 2020; H. Zhang et al., 2014; Liu et al., 2018; Qiu et al., 2019b; Zhang et al., 2019; Zhu et al., 2018). Even under the weak solar radiation conditions of winter, some local production of PAN occurs, which may be facilitated by high levels of VOC and NO_2 precursors in the atmosphere or rapid chemical reactions promoted by OH radicals (Hu et al., 2020; Liu et al., 2018; Wei et al., 2020; Zhang et al., 2019). Additionally, the high winter PAN level measured in Zhengzhou could be related to air mass transport from pollution source regions (Qiu et al., 2019b; Zhang et al., 2017). Frequent stagnant weather is not conducive to pollution dissipation (Meng et al., 2019), and PAN tends to accumulate under cold conditions, which prolong its atmospheric lifetime. Therefore, in contrast to our findings for summer photochemical pollution, the results from long-term measurement indicate that winter PAN pollution poses a major threat to Zhengzhou, as well as to the CPER urban agglomeration.

3.2. Comparison between urban and suburban areas

3.2.1. Temporal variations in PAN

During the study period, the highest average concentration of PAN was observed in winter (3.04 ± 2.06 ppbv) and the lowest was observed in summer (1.24 ± 0.77 ppbv) at the ZZU site (Table 1). At the GR site, the highest and lowest mean values of PAN occurred in spring (2.56 ± 1.66 ppbv) and summer (1.67 ± 1.25 ppbv), respectively. Fig. 2a shows the monthly variations in PAN at the ZZU and GR sites. The monthly pattern of PAN concentrations at the ZZU site followed a unimodal distribution with the highest 95th percentile (P95) value occurring in February, in accordance with the monthly $PM_{2.5}$ fluctuations (Fig. S2). By contrast, a multimodal pattern was observed at the GR site, with the highest mean and median concentrations both occurring in April. The median concentration of PAN was higher at ZZU than at GR from September to March, and the opposite trend occurred from April to August.

During autumn, the average and median concentrations of PAN were slightly higher at ZZU than at GR (Fig. 2b). The difference in PAN levels between the two sites was more significant in September than in the other months. Based on the elevated O_3 level at the ZZU site, active photochemical formation of PAN was promoted by sufficient ultraviolet (UV) radiation, and atmospheric stability might also have been a contributing factor (Rubio et al., 2007; Qiu et al., 2019a). We calculated the amount of PAN lost through thermal decomposition (TPAN; Fig. S3a) using a previously described method (Zhang et al., 2015), as the thermal stability of PAN increases with decreasing temperature and an increasing NO_2/NO ratio (Grosjean et al., 2002; Tuazon et al., 1991). Elevated values of suburban TPAN were observed at 13:00–16:00 local time (LT), indicating that little newly produced PAN was consumed, leading to greater accumulation in the local area in the afternoon at the ZZU site. The daily variations in NO_2/NO and temperature, shown in Fig. S3b and c, suggest that the effect of the lower NO_2/NO ratio outweighed the impact of temperature, leading to lower thermal stability of PAN at the GR site. As shown in Fig. 2a, in autumn, PAN at the GR site had elevated P95 values in October and November, which might be associated with pollution transport. As discussed further in Section 3.3.1, the contributions of PAN from distant sources were greater at the GR site (46% and 78%, respectively) than at the ZZU site (38% and 74%) in October and November.

During winter, the average, median, and P95 values of PAN at the ZZU site were significantly higher than the corresponding values at the GR site. In addition to the factors that cause elevated winter PAN concentrations, noted in Section 3.1, differences in PAN levels between urban and suburban areas in Zhengzhou may be associated with regional transport, as distant sources contributed approximately 90% of the total PAN. Details of the potential source regions and transport pathways are provided in Section 3.3.

During spring, suburban PAN levels were significantly enhanced in April and May, exceeding urban levels. Local sources dominated the observed PAN concentrations at both sites during these 2 months (greater than 60%; Section 3.3.1). The hourly average photolysis frequency of NO_2 (jNO_2) in spring was second to that in summer (Fig. S4), suggesting that sufficient solar radiation is available in spring to support photochemical reactions. The higher NO_2 level at the ZZU site than at the GR site did not appear to enhance PAN production. The increased concentration difference between the two sites around noon (10:00–16:00; Fig. S5) indicates that VOCs may act as the limiting factor for PAN formation at ZZU. Moreover, the average lifetimes of PAN in April and May were longer at the GR site (25.5 and 9.0 h, respectively) than at the ZZU site (24.8 and 5.9 h, respectively) according to the calculation results based on Eq. S4.

Summer saw the lowest PAN levels among the four seasons at both the ZZU and GR sites, which might be related to meteorological conditions. The shortest atmospheric lifetime for PAN occurred in summer (Fig. S6). Although strong solar radiation (illustrated by the highest seasonal jNO_2 level in Fig. S4) promoted the photochemical production of PAN, continuous high temperatures accelerated its thermal degradation (Fig. S7). Additionally, rainfall was abundant in Zhengzhou during summertime, reaching total seasonal precipitation levels of 41.5 and 110.7 mm at the ZZU and GR sites, respectively (Table S3). As suggested in previous studies (Hu et al., 2020; Qiu et al., 2020), precipitation may reduce the PAN level in summer by accelerating the wet removal of its precursors. Both sites were characterized by high RH in summer (Fig. S7). Salas et al. (2020) demonstrated that exposure to a humid environment increases the PAN degradation rate through heterogeneous reactions on the surfaces of some solid materials, promoting the removal of PAN in summer. Regional transport may also play a role in the observed seasonal differences. As illustrated in Section 3.3.1, locally generated PAN could have been transported away from the study area, reducing the measured PAN levels.

Based on these factors, we concluded that active PAN formation and strong thermal stability likely contributed to the high autumn PAN

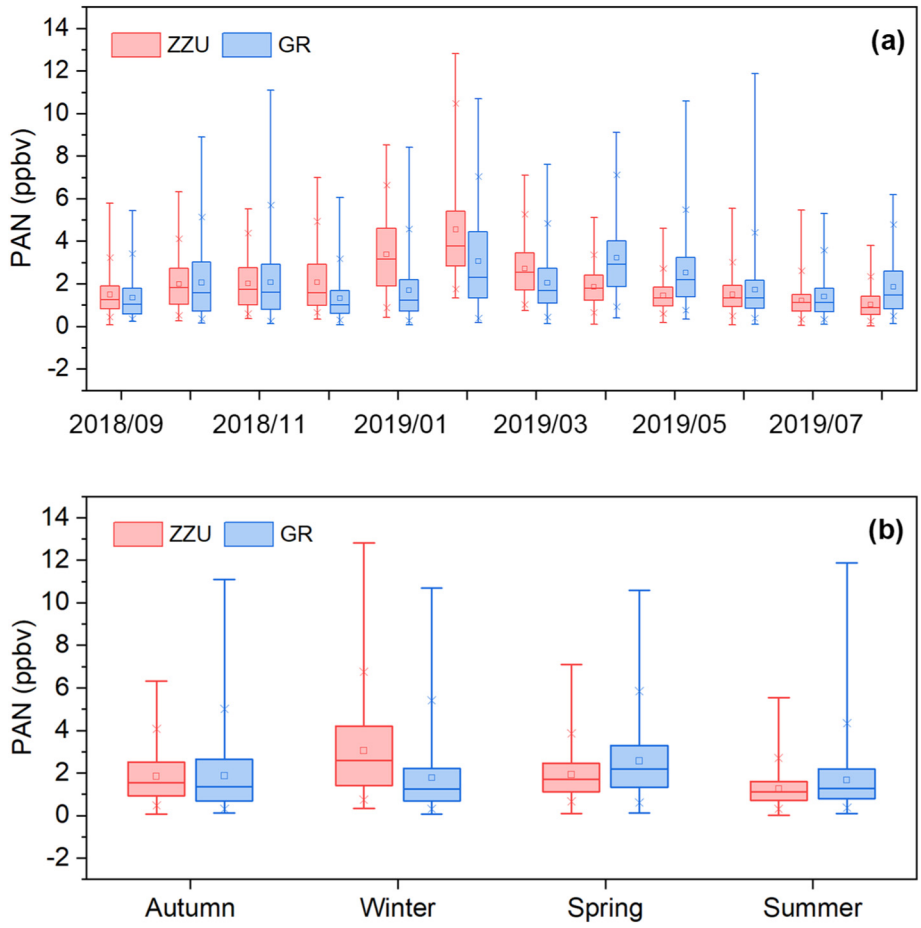

Fig. 2. Comparison of (a) monthly and (b) seasonal variations in PAN from September 2018 to August 2019 at the ZZU and GR sites in Zhengzhou. The horizontal line within each box represents the median, the dot represents the mean, upper and lower edges of the box represent the 75th and 25th percentiles, respectively, upper and lower limits of the vertical lines represent the maximum and minimum values, respectively, and upper and lower crosses indicate the 95th and 5th percentiles, respectively.

levels at ZZU. The low spring PAN levels at this site relative to GR could have been due to limited levels of VOC precursors and a shorter PAN lifetime. At both sites, the lowest PAN level occurred in summer and was associated with high temperature and RH, which are conducive to PAN decomposition. Seasonal differences in PAN concentrations between the two sites were also related to regional transport.

3.2.2. Relationship between pollutants and wind conditions

In this study, PAN and O_3 exhibited significant positive correlations ($p < 0.01$) in four seasons at both sites. At ZZU, the highest ($R = 0.54$) and lowest ($R = 0.37$) correlation coefficients were obtained for summer and winter, respectively. This seasonal correlation pattern (high R in summer and low R in winter) is in line with the expectation based on previous studies (Hu et al., 2020; G. Zhang et al., 2014). However, at the GR site, PAN was most strongly correlated with O_3 in winter ($R = 0.61$) among the four seasons. One possible reason for this difference is that significant daytime photochemical activity in February could have strengthened this positive correlation, as demonstrated by the high correlation coefficient ($R = 0.74$) for 11:00–16:00 LT. Additionally, the simultaneous rise in PAN and O_3 might be attributed to common transport from source regions (Zeng et al., 2019), highlighting the potential impact of wind conditions. PAN and $PM_{2.5}$ exhibited a significant positive correlation ($p < 0.01$) throughout the monitoring period, which was stronger at ZZU ($R = 0.60$) than at GR ($R = 0.29$). In terms of seasonality, the positive correlation coefficients were ranked as follows: winter (0.66 and 0.51 at ZZU and GR, respectively) > autumn (0.44 and 0.41) > spring (0.35 and 0.34) > summer (0.34 and 0.32). The high correlation between PAN and $PM_{2.5}$ was associated with their common sources, suggesting the non-negligible role of atmospheric oxidation capacity. During winter, compared to periods of calm wind (WS slower than 1 m/s), the positive correlation coefficients for PAN and $PM_{2.5}$ increased significantly, to 0.84 and 0.70 at ZZU and GR, respectively, at high WSs (faster than 1 m/s). This result indicates that the simultaneous transport of PAN and $PM_{2.5}$ promotes a strong correlation between them, which is facilitated by the long atmospheric lifetime of PAN under low-temperature conditions.

To elucidate the effect of wind conditions on the correlation between PAN and O_3 (and between PAN and $PM_{2.5}$), we further explored pollutant concentrations using polar coordinates relating pollutant levels to WS and wind direction (Fig. 3). The prevailing winds in winter were from the WNW and ENE sectors and from the WNW and SE sectors at the ZZU and GR sites, respectively (Fig. S8). As shown in Fig. 3, high PAN concentrations were associated with increased prevalence of ENE winds (2–3 m/s) and E winds (approximately 2.0–2.5 m/s) at the ZZU site. By contrast, high O_3 values occurred in tandem with southeasterly wind conditions at WSs of 2 m/s. These results revealed that when the ZZU site was affected by air masses arriving from different directions, the PAN level was decoupled from the O_3 concentration in any given direction. Moreover, low concentrations of O_3 and high concentrations of NO were observed with a low WS (slower than 1 m/s), suggesting that the NO titration effect caused by intense local vehicle emissions significantly increased the decomposition of O_3. O_3 production was also suppressed in winter due to low UV intensity (Fig. S4). In contrast to O_3, moderate to high concentrations of PAN were observed at low WSs. This enhancement of PAN occurs because the local formation of PAN is not as dependent as O_3 formation on UV intensity (Zhang et al., 2019).

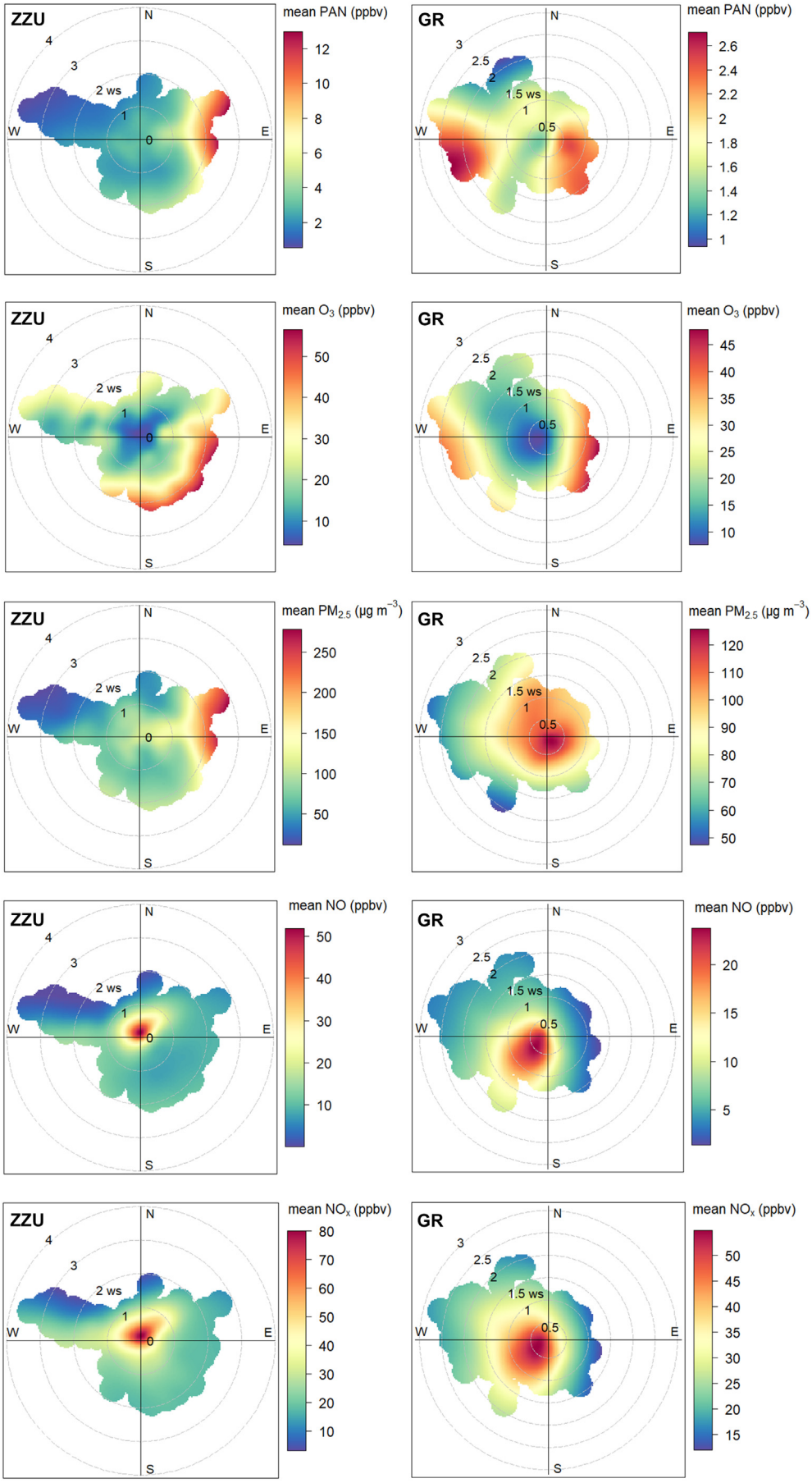

Fig. 3. Polar plots of pollutant concentrations during winter at the ZZU and GR sites.

These reasons may partly explain the weak correlation between PAN and O_3 at the ZZU site in winter.

At GR, high concentrations of PAN and O_3 simultaneously occurred with moderate speeds of prevailing SE and ESE winds (approximately 1.0–1.5 m/s) and higher speeds of W and WNW winds (2.0–2.5 m/s). Enhanced photochemical production undoubtedly occurs during daytime at high prevailing WSs in the presence of sufficient precursors. Nevertheless, the strong correlation at the GR site in winter might have been driven in part by the transport of air masses containing high levels of PAN and O_3. These air masses originated from areas to the west and west-northwest of the GR site with intensive anthropogenic activities and the Zhengzhou city center (southeast of the GR site).

High concentrations of both PAN and $PM_{2.5}$ occurred under a moderate prevailing ENE wind (2–3 m/s) at the ZZU site. Low concentrations of both pollutants were associated with a relatively high-speed prevailing WNW wind (above 3 m/s). This pattern suggests that the significant correlation between PAN and $PM_{2.5}$ at the ZZU site was affected by the transport of air masses that were either enriched or lacking in both PAN and $PM_{2.5}$ from specific directions. At the GR site, high values of PAN and $PM_{2.5}$ did not occur with WSs higher than 2 m/s. Nevertheless, moderate winds (1–2 m/s) from westerly directions (from WNW to WSW) were related to moderate pollutant levels. This result suggests that short-distance (corresponding to moderate WSs) co-transport was more conducive to consistency between PAN and $PM_{2.5}$ levels.

In summary, PAN and O_3 were weakly correlated at the ZZU site due to NO titration, PAN enhancement, and air masses arriving from multiple directions. The strong positive correlations between PAN and $PM_{2.5}$ in winter at both sites were related to their joint transport from specific directions. Similar transport characteristics promoted the unexpected positive correlation between PAN and O_3 at the GR site.

3.3. Source analysis and regional transport

3.3.1. Contribution of local and distant PAN sources

The measured PAN values result from a combination of various sources and sinks. In brief, PAN levels can be enhanced through local formation and regional transport inflow. Thermal decomposition (and other removal pathways) and transport outflow can reduce the observed PAN levels. Here, we employed a previously described calculation method (Wang et al., 2015) to determine the monthly production and decomposition of PAN and the contributions of local and distant PAN sources in Zhengzhou. Detailed information about the calculation process is provided in Supporting Information S5.

Fig. 4 shows monthly source analysis results for PAN in Zhengzhou. At the ZZU site, local production of PAN decreased gradually from September to January and increased from February to July. The suburban site exhibited a trend similar to that for the urban area, but with differing fluctuations in May and June. With the shift from summer to autumn, local production of PAN was reduced due to the effects of meteorological factors and precursor concentrations. As a result, a sudden decrease in local PAN production was observed in August at both sites. During the study period, local sources contributed 65.9% and 66.8% of the PAN at the ZZU and GR sites, respectively. From November to March, PAN pollution at both sites was dominated by regional transport, and PAN inflow contributed to more than 50% of the total PAN during these five cold months. In particular, the proportion of distant-source PAN was elevated during the 3 months of winter (88%–94%).

Based on the source estimation results and prevailing wind conditions, we analyzed potential transport between urban and suburban areas of Zhengzhou. In contrast to the findings of Wang et al. (2015), distant-source PAN showed negative values at both sites during summer. This result suggests that PAN produced in situ may be transported outward, as thermal decomposition is the only PAN loss pathway. The average lifetime of PAN in summer was 3.5 h based on Eq. S4. When the urban area was dominated by southeasterly winds (WS of approximately 1–3 m/s; see wind frequency diagram in Fig. S8), PAN could be transported approximately 12.6–37.8 km. As the GR site was located approximately 12 km NW of the ZZU site, the PAN level at the GR site was affected by PAN outflow from the urban area. By contrast, PAN outflow from the GR site rarely had an effect on the urban site in summer. The reason for this discrepancy was the decrease in average hourly WS (1–2 m/s; Fig. S8) when wind from northwesterly directions prevailed at the GR site. PAN transport from ZZU to GR was also demonstrated by PAN inflow at GR, as determined from the calculation results for summer presented in Fig. 4, whereas no PAN inflow occurred at ZZU.

3.3.2. Cluster and potential source contribution function analyses

As noted above, PAN levels in Zhengzhou were significantly affected by regional transport during the cold months. Therefore, using ZZU as the receptor site, we conducted cluster analysis to determine the air mass transport pathways and compare air mass characteristics (Wei et al., 2020; Zhang et al., 2017). Potential source contribution function (PSCF) analysis was also performed to identify the geographic location and spatial distribution of source regions affecting the ZZU site (Ashbaugh et al., 1985; Ding et al., 2020). The method and parameters used for air mass cluster analysis and PSCF calculations are detailed in Supporting Information S6.

As shown in Fig. 5, the major trajectories were divided into three categories for each month. At the end of autumn (November), Cluster I originated from the SE of Henan and accounted for the largest number of trajectories (48.4%). This air mass was characterized by short-distance transport within Henan Province and was associated with the majority of the PAN pollution trajectories (65.5%; Table S4). Similar proportions of PAN pollution trajectories associated with Clusters II and III (34.4% and 35.1%, respectively) suggest secondary effects relative to Cluster I. Clusters II and III were influenced by air masses from the northwest (Shanxi and Shaanxi Province) and northeast (Shandong Province), respectively.

In December (56.2%), the dominant air mass originated from southern Hebei Province and passed through western Shandong Province. By contrast, the most important air masses in the other 2 months originated from eastern Henan Province (45.3% and 49.0%, respectively). As shown in Table S4, the numbers of PAN pollution trajectories were high for these dominant air masses, with proportions of 69.8% (Cluster I), 77.6% (Cluster II), and 55.0% (Cluster II) in December, January, and February, respectively. Additionally, the air masses contributing to relatively small proportions of PAN pollution were from the north (Cluster II, 17.9%), northeast (Cluster III, 6.3%), and northwest (Cluster III, 30.8%) in December, January, and February, respectively. Relatively clean air masses arrived in December and January from Inner Mongolia, and in February from southern Shanxi Province.

At the beginning of spring (March), the dominant air mass (Cluster I; 73.1%) was from the south and was characterized by very short-distance transport within Henan Province. Cluster I was associated with the largest proportion of PAN pollution trajectories (63.5%; Table S4). By contrast, the air masses represented by Clusters II and III, which originated from the northwestern (from Shaanxi) and northeastern (from Hebei) directions, were transported over longer distances and were relatively cleaner, accounting for only 16.7% and 14.3% of the PAN pollution trajectories, respectively.

A high weighted PSCF (WPSCF) value indicates that the grid area has a strong impact on the sampling site (Zhang et al., 2017). As shown in Fig. 5, in November, potential source regions with high WPSCF values (>0.6) were located approximately 40 km and 90–130 km southeast and 60–100 km northeast of the ZZU site. Likewise, a region with a high WPSCF value (>0.6) southeast of the ZZU site was present in December, and another region appeared at a distance of 175–200 km (northern Anhui Province). Other regions with high WPSCF values during December were located approximately 25–65 km east and 25 km southwest of ZZU. In January, compared with November and December, a larger and closer pollution source region (WPSCF >0.7) was located southeast of the sampling site at distances of 20–60 km. Two additional

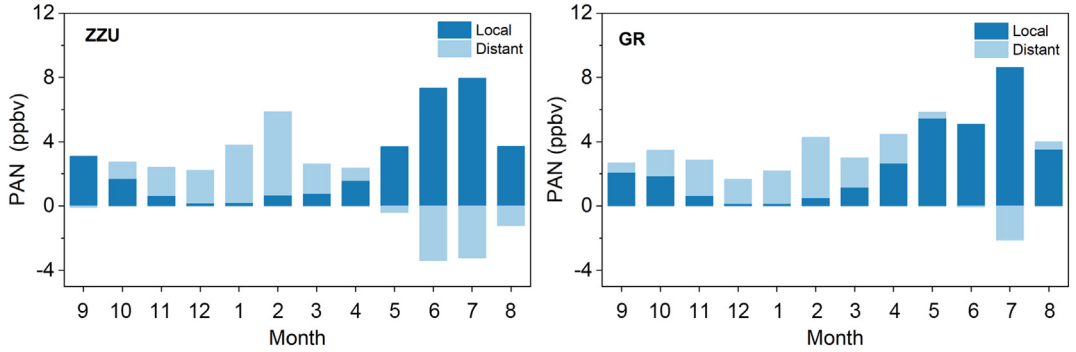

Fig. 4. PAN from local and distant sources at the ZZU and GR sites during daytime (08:00–18:00 LT).

regions had high WPSCF values; they were situated 55 km northeast and 50–90 km northwest of the sampling location. In February, the WPSCF values of regions located 90–140 km to the east, 20–40 km and 90–110 km to the northeast, and 7–20 km to the southwest were higher than 0.6. The results in March differed from those obtained in the previous 4 months. Regions with WPSCF values higher than 0.5

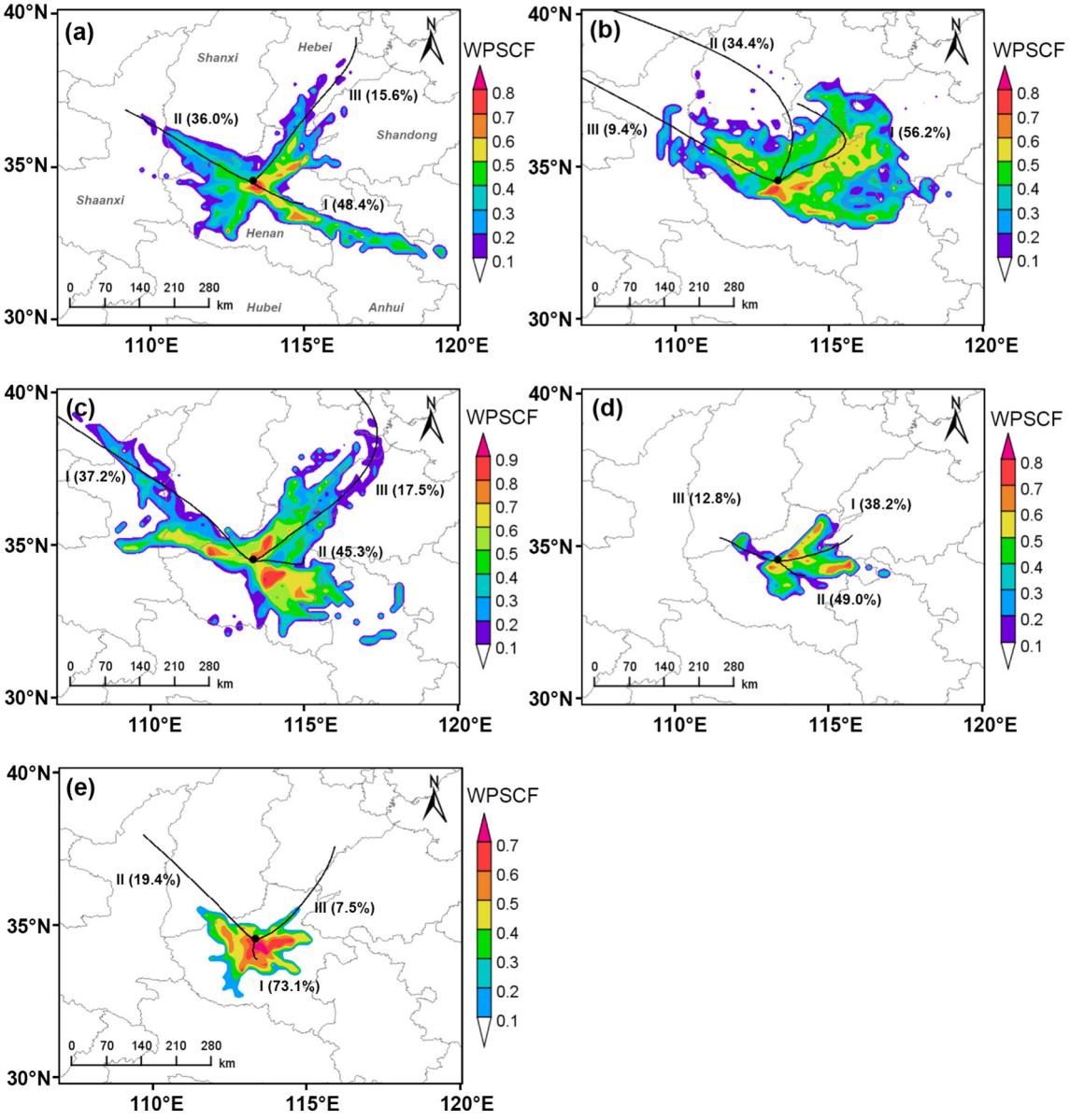

Fig. 5. Results of cluster and PSCF analyses for (a) November, (b) December, (c) January, (d) February, and (e) March at the ZZU site in Zhengzhou. The simulation period for February was from the 16th to the 28th to minimize uncertainties related to changes in anthropogenic activities during the Chinese Lunar New Year holiday (Ye et al., 2016). The proportions indicate the contributions of specific clusters to the total trajectories.

were located within a radius of 50–80 km of the ZZU site from the east clockwise to the southwest. A region 35–50 km to the west also contributed to PAN pollution at ZZU.

Therefore, in cold months, potential distant source regions of PAN at the ZZU site were located within Henan Province in all directions except for the northwest. Elucidating the regional interactions between Zhengzhou and the surrounding cities, especially cities in the northeast of Henan Province (Xinxiang, Hebi, and Anyang), cities to the east (Kaifeng and Shangqiu), and cities from the southeast to the southwest (Zhoukou, Xuchang, and Pingdingshan) of the study area, could help improve PAN pollution in Zhengzhou during cold months.

3.4. Impacts of air mass characteristics on PAN and O_3

In this section, we aim to clarify how different air masses affect the relationship between PAN and O_3 based on the statistical results of cluster analysis. The average levels of pollutants and meteorological parameters corresponding to specific clusters are shown in Table 2. Detailed results on the direction, speed, and height of clustered backward trajectories are presented in Fig. S9. Longer trajectories correspond to faster-moving air masses (Malley et al., 2016). In each month, relative to the other two clusters, PAN and O_3 corresponding to the focal cluster may have higher or lower average concentrations. Based on these differences, we established the following four groups based on characteristics of PAN and O_3 and the cluster analysis outcomes for each month: (1) high PAN-high O_3 (November), (2) high PAN-low O_3 (December and January), (3) low PAN-low O_3 (February), and (4) low PAN-high O_3 (March).

Representing Group 1, high PAN-high O_3 conditions occurred in November. The average concentrations of PAN and O_3 were higher in Cluster I than in the other clusters, and the concentrations of most other pollutants (except for NO and SO_2) were also high. On the diagram of trajectory height (Fig. S9), Cluster I corresponds to a low-height and relatively slow-moving air mass, which carried air from heavily polluted areas along its transport pathway to the ZZU site. During transport, primary pollutants such as NO and SO_2 may be converted or removed due to the strong atmospheric photochemical oxidation effect.

High PAN-low O_3 (i.e., Group 2) conditions were observed in December and January. The O_3 concentration was significantly lower for Cluster I in December than for the other two clusters, whereas the concentrations of PAN, other trace gases, and $PM_{2.5}$ exhibited the opposite pattern. Similar pollution characteristics were also observed for Cluster II in January. For Clusters I and II in December and January, relatively high NO concentrations promoted decreased O_3 due to titration reactions, whereas PAN accumulated due to the low temperatures of the air masses. These two clusters both originated from the east and were characterized by low height from the ground surface, low speed, low temperature, and high RH. These characteristics suggest that the meteorological conditions were conducive to the transport of secondary pollutants and hygroscopic growth of aerosols (Li et al., 2017), possibly driving the significant increases (1.6–2.1-fold) in $PM_{2.5}$ for Clusters I and II in December and January, respectively.

Low PAN-low O_3 (i.e., Group 3) conditions occurred in February. The air mass of Cluster III was derived from a high altitude, in contrast to the other two clusters. CO, a relatively inert primary pollutant, had similar concentrations in all three clusters. The SO_2 level in Cluster III was elevated, and the average concentration of NO_X was reduced, relative to the other two air masses. These results suggest that although the speed of the air mass representing Cluster III was slow, photochemical activity might be weak due to insufficient precursor levels or meteorological conditions. Therefore, O_3 and PAN remained at low levels in Cluster III.

March was characterized by low PAN-high O_3 (i.e., Group 4) conditions. PAN was reduced through thermal decomposition due to the high temperatures of the air masses in Cluster II. Relative to the other two clusters, the SO_2, CO, and NO_X characteristics of Cluster II for this Group were similar to the characteristics of Group 3, although O_3 was less likely to be enhanced by strong photochemical reactions in Cluster II. Thus, the increase in O_3 concentration might have been driven by two factors: the weakened titration reaction caused by lower NO levels, and high O_3 content in air masses rapidly moving downward from a high altitude.

Based on the findings discussed above, we made the following conclusions. When the PAN and O_3 concentrations corresponding to a specific air mass were concurrently high or low (November and March), the air mass was characterized by low speed. However, the initial heights of the air masses differed. Air masses derived from low altitudes tended to have increased PAN and O_3 due to stronger photochemical activities relative to air masses from high altitudes. On the other hand, when the PAN and O_3 concentrations of a specific air mass exhibited opposite trends (December, January, and February), the sink pathways of PAN and O_3 played important roles, and high-altitude O_3 injection might also occur.

3.5. Limitations

We note that this study has some limitations. First, we estimated the average hourly peroxyacetyl (PA) radical level based on assumed steady atmospheric conditions when calculating the contributions of local and distant PAN sources. This assumption might have caused some uncertainty, as PA levels were assumed to be constant throughout each month. Nevertheless, monthly variations can still be discussed in the context of this study. Second, as the estimation of thermal decomposition does not consider the loss of PA radicals to NO or other free radicals (LaFranchi et al., 2009), the PA and PAN production rates estimated here are theoretical maximum values, and the contributions of distant sources were theoretical minimum values. Third, VOC compounds, important precursors of PAN, have regional transport sources in the NCP (Li et al., 2020). However, as VOCs were not continuously measured in

Table 2
Average concentrations (or levels) of PAN (ppbv), O_3 (ppbv), NO_X (ppbv), SO_2 (ppbv), CO (ppmv), $PM_{2.5}$ (μg/m^3), Temp (°C), and RH (%) for all clusters.

Group number	Month	Cluster	PAN	O_3	NO	NO_2	SO_2	CO	$PM_{2.5}$	Temp	RH
Group 1	November	I	2.3	17.3	26.1	26.7	3.4	1.3	95.4	11.1	69.1
		II	1.7	15.8	26.8	26.6	3.8	1.1	83.3	11.3	59.1
		III	1.7	13.0	5.0	18.6	2.9	0.9	68.4	8.7	72.2
Group 2	December	I	2.6	7.6	23.4	28.5	4.5	1.1	102.6	3.0	57.6
		II	1.3	8.1	16.3	22.2	4.0	0.7	63.9	2.4	41.8
		III	1.5	15.5	16.6	25.3	4.4	0.4	57.8	8.9	27.5
	January	I	3.0	14.2	29.9	20.1	4.1	1.1	79.6	3.9	40.2
		II	4.3	8.9	43.8	31.0	5.1	1.2	126.9	2.2	59.3
		III	2.1	11.0	33.9	17.9	3.9	0.8	59.4	1.2	43.4
Group 3	February	I	5.0	21.6	24.2	10.1	3.4	1.3	133.6	4.6	62.3
		II	4.8	26.4	25.2	9.9	3.6	1.1	126.3	6.5	62.8
		III	3.6	19.7	15.1	9.0	3.6	1.2	119.4	5.4	66.6
Group 4	March	I	3.1	27.7	16.4	7.0	3.7	0.5	71.4	13.1	52.6
		II	1.7	29.0	13.1	5.9	3.5	0.7	32.8	14.8	27.9
		III	2.1	26.8	13.8	6.2	2.9	0.4	46.3	10.0	34.6

the present study, we could discuss only the contributions and geographical origins of regional PAN sources. Further investigation of the predominant VOC species responsible for PAN formation, including their spatiotemporal variations and source apportionment, is needed to clarify the impacts of regional transport on PAN and the relationships among pollutants.

4. Conclusion

In this study, the first measurement campaign of atmospheric PAN at urban and suburban sites in Zhengzhou was conducted for 1 year. At the urban site, there was less severe summer PAN pollution (average value: 1.24 ppbv) than was reported in previous studies. However, at the suburban site, there was greater summertime PAN formation activity (average: 1.67 ppbv) than in other regions of China. Winter PAN levels at the two sites (average: 3.04 and 1.77 ppbv) were higher than the concentrations reported in previous short-term studies. PAN levels were higher at the urban site than at the suburban site during autumn and winter, with this difference driven by active PAN formation, thermal decomposition, PAN lifetime, and regional PAN inflows. In spring and summer, the average levels of PAN at the suburban site were greater, and PAN precursors and local meteorological factors that affect formation and removal pathways likely played important roles. According to the results of source apportionment, PAN was dominated by local production from April to October and by regional transport from November to March at both the urban and suburban sites in Zhengzhou. From November 2018 to March 2019, air masses with high PAN concentrations were characterized by short-distance transport. Polluted air masses originated from the east, south, and southeast of Henan Province, and from southern Hebei Province. The results of PSCF analysis suggest that regional transport occurred from source areas within Henan Province in directions other than the northwest. Therefore, the reduction of PAN pollution would rely heavily on effective cooperation between the study locality (Zhengzhou) and eight surrounding cities (Xinxiang, Hebi, Anyang, Kaifeng, Shangqiu, Zhoukou, Xuchang, and Pingdingshan).

Co-transport may drive the association of PAN levels with those of O_3 and $PM_{2.5}$. At the suburban site, PAN was most strongly correlated with O_3 in winter (Pearson correlation coefficient, $R = 0.61$), which was related to air masses from the city center and from west and west-northwest of the suburban site. Driven by ENE and WNW winds at the urban site and WSW winds at the suburban site, the correlation between PAN and $PM_{2.5}$ was strongest in winter at both sites ($R = 0.66$ and 0.51, respectively). According to the cluster analysis results, we identified four groups based on characteristics of PAN and O_3 that corresponded to specific air masses. Features of air masses that reached the urban site in Zhengzhou (including pollutant contents and meteorological characteristics) affected the consistency between PAN and O_3 trends. Unfortunately, as the atmospheric abundance of VOC precursors was not monitored in this study, accurately determining the intensity of photochemical reactions or secondary aerosol formation during transport from different directions was not possible. Despite this shortcoming, the current results indicate that the correlations of PAN with $PM_{2.5}$ and O_3 have potential for tracing air pollution introduced to an area from surrounding industrial cities.

This study suggests that controlling the emission of PAN precursors in the surrounding cities is of great benefit to improving air quality in Zhengzhou. NO_X and VOC emissions from combustion and mobile sources are recommended to be reduced by upgrading and transforming the iron/steel industry and changing vehicle engine types. Besides, stringent supervision of VOC emissions from key industries such as process and solvent sources is required to be implemented.

CRediT authorship contribution statement

Mei Sun: Investigation, Writing – original draft. **Ying Zhou:** Writing – review & editing. **Yifei Wang:** Formal analysis. **Xiaochen Zheng:** Formal analysis. **Jia'nan Cui:** Data curation, Writing – review & editing. **Dong Zhang:** Data curation. **Jianbo Zhang:** Funding acquisition, Supervision. **Ruiqin Zhang:** Funding acquisition, Resources.

Declaration of competing interest

The authors declare that they have no known competing financial interests or personal relationships that could have appeared to influence the work reported in this paper.

Acknowledgments

This work was supported by the National Key Research and Development Program of China (grant number: 2017YFC0212400). The authors thank Jinshuai Zhao, Shenbo Wang, Shijie Yu, and Youchang Sun for their kind help with equipment maintenance.

Appendix A. Supplementary data

Supplementary data to this article can be found online at https://doi.org/10.1016/j.scitotenv.2021.147303.

References

An, Z., Huang, R.J., Zhang, R., Tie, X., Li, G., Cao, J., Zhou, W., Shi, Z., Han, Y., Gu, Z., Ji, Y., 2019. Severe haze in northern China: a synergy of anthropogenic emissions and atmospheric processes. Proc. Natl. Acad. Sci. USA 116, 8657–8666.

Ashbaugh, L.L., Malm, W.C., Sadeh, W.Z., 1985. A residence time probability analysis of sulfur concentrations at Grand Canyon National Park. Atmos. Environ. 19, 1263–1270.

Crowley, J.N., Pouvesle, N., Phillips, G.J., Axinte, R., Fischer, H., Petäjä, T., Nölscher, A., Williams, J., Hens, K., Harder, H., Martinez-Harder, M., Novelli, A., Kubistin, D., Bohn, B., Lelieveld, J., 2018. Insights into HO_X and RO_X chemistry in the boreal forest via measurement of peroxyacetic acid, peroxyacetic nitric anhydride (PAN) and hydrogen peroxide. Atmos. Chem. Phys. 18, 13457–13479.

CSY, 2019. China Statistical Yearbook. China Statistical Publishing House, Beijing.

Dassau, T.M., Shepson, P.B., Bottenheim, J.W., Ford, K.M., 2004. Peroxyacetyl nitrate photochemistry and interactions with the Arctic surface. J. Geophys. Res. Atmos. 109.

DeMarini, D.M., Shelton, M.L., Kohan, M.J., Hudgens, E.E., Kleindienst, T.E., Ball, L.M., Walsh, D., de Boer, J.G., Lewis-Bevan, L., Rabinowitz, J.R., Claxton, L.D., Lewtas, J., 2000. Mutagenicity in lung of Big Blue® mice and induction of tandem-base substitutions in Salmonella by the air pollutant peroxyacetyl nitrate (PAN): predicted formation of intrastrand cross-links. Mutat. Res.-Fund. Mol. M. 457, 41–55.

Ding, M., Tian, B., Ashley, M., Zhu, Z., Wang, L., Yang, S., Li, C., Xiao, C., Qin, D., 2020. Year-round record of near-surface ozone and "O_3 enhancement events" (OEEs) at Dome A, East Antarctica. Atmos. Chem. Phys. Discuss. 2020, 1–34.

Fischer, E.V., Jacob, D.J., Yantosca, R.M., Sulprizio, M.P., Millet, D.B., Mao, J., Paulot, F., Singh, H.B., Roiger, A., Ries, L., Talbot, R.W., Dzepina, K., Pandey Deolal, S., 2014. Atmospheric peroxyacetyl nitrate (PAN): a global budget and source attribution. Atmos. Chem. Phys. 14, 2679–2698.

Gao, T., Han, L., Wang, B., Yang, G., Xu, Z., Zeng, L., Zhang, J., 2014. Peroxyacetyl nitrate observed in Beijing in August from 2005 to 2009. J. Environ. Sci. 26, 2007–2017.

Grosjean, E., Grosjean, D., Woodhouse, L.F., Yang, Y.J., 2002. Peroxyacetyl nitrate and peroxypropionyl nitrate in Porto Alegre, Brazil. Atmos. Environ. 36, 2405–2419.

Han, J., Lee, M., Shang, X., Lee, G., Emmons, L.K., 2017. Decoupling peroxyacetyl nitrate from ozone in Chinese outflows observed at Gosan Climate Observatory. Atmos. Chem. Phys. 17, 10619–10631.

Hu, B., Liu, T., Hong, Y., Xu, L., Li, M., Wu, X., Wang, H., Chen, J., Chen, J., 2020. Characteristics of peroxyacetyl nitrate (PAN) in a coastal city of southeastern China: photochemical mechanism and pollution process. Sci. Total Environ. 719, 137493.

Khan, M.A.H., Cooke, M.C., Utembe, S.R., Archibald, A.T., Derwent, R.G., Jenkin, M.E., Leather, K.E., Percival, C.J., Shallcross, D.E., 2017. Global budget and distribution of peroxyacetyl nitrate (PAN) for present and preindustrial scenarios. Int. J. Earth. Environ. Sci. 2, 130.

Kotchenruther, R.A., Jaffe, D.A., Jaeglé, L., 2001. Ozone photochemistry and the role of peroxyacetyl nitrate in the springtime northeastern Pacific troposphere: results from the Photochemical Ozone Budget of the Eastern North Pacific Atmosphere (PHOBEA) campaign. J. Geophys. Res. Atmos. 106, 28731–28742.

LaFranchi, B.W., Wolfe, G.M., Thornton, J.A., Harrold, S.A., Browne, E.C., Min, K.E., Wooldridge, P.J., Gilman, J.B., Kuster, W.C., Goldan, P.D., de Gouw, J.A., McKay, M., Goldstein, A.H., Ren, X., Mao, J., Cohen, R.C., 2009. Closing the peroxy acetyl nitrate budget: observations of acyl peroxy nitrates (PAN, PPN, and MPAN) during BEARPEX 2007. Atmos. Chem. Phys. 9, 7623–7641.

Lee, J.B., Yoon, J.S., Jung, K., Eom, S.W., Chae, Y.Z., Cho, S.J., Kim, S.D., Sohn, J.R., Kim, K.H., 2013. Peroxyacetyl nitrate (PAN) in the urban atmosphere. Chemosphere 93, 1796–1803.

Lefohn, A.S., Malley, C.S., Smith, L., Wells, B., Hazucha, M., Simon, H., Naik, V., Mills, G., Schultz, M.G., Paoletti, E., De Marco, A., Xu, X., Zhang, L., Wang, T., Neufeld, H.S., Musselman, R.C., Tarasick, D., Brauer, M., Feng, Z., Tang, H., Kobayashi, K., Sicard, P., Solberg, S., Gerosa, G., 2018. Tropospheric ozone assessment report: global ozone

metrics for climate change, human health, and crop/ecosystem research. Elementa-Sci. Anthrop. 6.
Li, L., Tan, Q., Zhang, Y., Feng, M., Qu, Y., An, J., Liu, X., 2017. Characteristics and source apportionment of $PM_{2.5}$ during persistent extreme haze events in Chengdu, southwest China. Environ. Pollut. 230, 718–729.
Li, Q., Su, G., Li, C., Liu, P., Zhao, X., Zhang, C., Sun, X., Mu, Y., Wu, M., Wang, Q., Sun, B., 2020. An investigation into the role of VOCs in SOA and ozone production in Beijing, China. Sci. Total Environ. 720, 137536.
Li, B., Ho, S.S.H., Qu, L., Gong, S., Ho, K.F., Zhao, D., Qi, Y., Chan, C.S., 2021. Temporal and spatial discrepancies of VOCs in an industrial-dominant city in China during summertime. Chemosphere 264, 128536.
Lin, J.K., Chen, K.J., Liu, G.Y., Chu, Y.R., Lin-Shiau, S.Y., 2000. Nitration and hydoxylation of aromatic amino acid and guanine by the air pollutant peroxyacetyl nitrate. Chem. Biol. Interact. 127, 219–236.
Liu, L., Wang, X., Chen, J., Xue, L., Wang, W., Wen, L., Li, D., Chen, T., 2018. Understanding unusually high levels of peroxyacetyl nitrate (PAN) in winter in urban Jinan, China. J. Environ. Sci. 71, 249–260.
Malley, C.S., Cape, J.N., Jones, M.R., Leeson, S.R., Coyle, M., Braban, C.F., Heal, M.R., Twigg, M.M., 2016. Regional and hemispheric influences on measured spring peroxyacetyl nitrate (PAN) mixing ratios at the Auchencorth UK EMEP supersite. Atmos. Res. 174-175, 135–141.
Meng, C., Cheng, T., Gu, X., Shi, S., Wang, W., Wu, Y., Bao, F., 2019. Contribution of meteorological factors to particulate pollution during winters in Beijing. Sci. Total Environ. 656, 977–985.
Moravek, A., Stella, P., Foken, T., Trebs, I., 2015. Influence of local air pollution on the deposition of peroxyacetyl nitrate to a nutrient-poor natural grassland ecosystem. Atmos. Chem. Phys. 15, 899–911.
Payne, V.H., Fischer, E.V., Worden, J.R., Jiang, Z., Zhu, L., Kurosu, T.P., Kulawik, S.S., 2017. Spatial variability in tropospheric peroxyacetyl nitrate in the tropics from infrared satellite observations in 2005 and 2006. Atmos. Chem. Phys. 17, 6341–6351.
Qiu, Y., Lin, W., Li, K., Chen, L., Yao, Q., Tang, Y., Ma, Z., 2019a. Vertical characteristics of peroxyacetyl nitrate (PAN) from a 250-m tower in northern China during September 2018. Atmos. Environ. 213, 55–63.
Qiu, Y., Ma, Z., Li, K., 2019b. A modeling study of the peroxyacetyl nitrate (PAN) during a wintertime haze event in Beijing, China. Sci. Total Environ. 650, 1944–1953.
Qiu, Y., Ma, Z., Lin, W., Quan, W., Pu, W., Li, Y., Zhou, L., Shi, Q., 2020. A study of peroxyacetyl nitrate at a rural site in Beijing based on continuous observations from 2015 to 2019 and the WRF-Chem model. Front. Env. Sci. Eng. 14, 71.
Roberts, J.M., 2007. PAN and Related Compounds. Volatile Organic Compounds in the Atmosphere. Blackwell Publishing, Oxford, UK, pp. 221–268.
Rubio, M., Gramsch, E., Lissi, E., Villena, G., 2007. Seasonal dependence of peroxyacetyl nitrate (PAN) concentrations in downtown Santiago, Chile. Atmósfera 20, 319–328.
Salas, J., Burgos Paci, M.A., Malanca, F.E., 2020. Water vapour influence over the PAN stability: homogeneous and heterogeneous processes between PAN-NO_2-H_2O. Atmos. Environ. 232, 117537.
Stephens, E.R., 1969. The formation, reaction, and properties of peroxyacetyl nitrates (PANs) in photochemical air pollution. Adv. Environ. Sci. Technol. 1, 119–146.
Sun, M., Cui, J.N., Zhao, X., Zhang, J., 2020. Impacts of precursors on peroxyacetyl nitrate (PAN) and relative formation of PAN to ozone in a southwestern megacity of China. Atmos. Environ. 231, 117542.
Taylor, O.C., 1969. Importance of peroxyacetyl nitrate (PAN) as a phytotoxic air pollutant. J. Air Pollut. Control Assoc. 19, 347–351.
Tuazon, E.C., Carter, W.P.L., Atkinson, R., 1991. Thermal decomposition of peroxyacetyl nitrate and reactions of acetyl peroxy radicals with NO and NO_2 over the temperature range 283–313 K. J. Phys. Chem. 95, 2434–2437.
Vyskocil, A., Viau, C., Lamy, S., 1998. Peroxyacetyl nitrate: review of toxicity. Hum. Exp. Toxicol. 17, 212–220.
Wang, S., Hao, J., 2012. Air quality management in China: issues, challenges, and options. J. Environ. Sci. 24, 2–13.
Wang, B., Shao, M., Roberts, J., Yang, G., Yang, F., Hu, M., Zeng, L., Zhang, Y., Zhang, J., 2010. Ground-based on-line measurements of peroxyacetyl nitrate (PAN) and peroxypropionyl nitrate (PPN) in the Pearl River Delta, China. Int. J. Environ. Anal. Chem. 90, 548–559.
Wang, B.G., Zhu, D., Zou, Y., Wang, H., Zhou, L., Ouyang, X., Shao, H.F., Deng, X.J., 2015. Source analysis of peroxyacetyl nitrate (PAN) in Guangzhou, China: a yearlong observation study. Atmos. Chem. Phys. Discuss. 2015, 17093–17133.
Wang, H., Zhao, L., Xie, Y., Hu, Q., 2016. "APEC blue"-the effects and implications of joint pollution prevention and control program. Sci. Total Environ. 553, 429–438.
Wang, X., Wang, T., Xue, L., Nie, W., Xu, Z., Poon, S.C.N., Wang, W., 2017. Peroxyacetyl nitrate measurements by thermal dissociation–chemical ionization mass spectrometry in an urban environment: performance and characterizations. Front. Env. Sci. Eng. 11, 3.
Wang, S., Yin, S., Zhang, R., Yang, L., Zhao, Q., Zhang, L., Yan, Q., Jiang, N., Tang, X., 2019. Insight into the formation of secondary inorganic aerosol based on high-time-resolution data during haze episodes and snowfall periods in Zhengzhou, China. Sci. Total Environ. 660, 47–56.
Wei, W., Zang, J., Wang, X., Cheng, S., 2020. Peroxyacetyl nitrate (PAN) in the border of Beijing, Tianjin and Hebei of China: concentration, source apportionment and photochemical pollution assessment. Atmos. Res. 246, 105106.
WHO, 1987. WHO Air Quality Guideline for Europe. Air Quality Guidelines for Europe. WHO Regional Office in Europe, Copenhagen.
Wolfe, G.M., Thornton, J.A., McNeill, V.F., Jaffe, D.A., Reidmiller, D., Chand, D., Smith, J., Swartzendruber, P., Flocke, F., Zheng, W., 2007. Influence of trans-Pacific pollution transport on acyl peroxy nitrate abundances and speciation at Mount Bachelor Observatory during INTEX-B. Atmos. Chem. Phys. 7, 5309–5325.
Xiao, H., Huang, Z., Zhang, J., Zhang, H., Chen, J., Zhang, H., Tong, L., 2017. Identifying the impacts of climate on the regional transport of haze pollution and inter-cities correspondence within the Yangtze River Delta. Environ. Pollut. 228, 26–34.
Xu, Z., Zhang, J., Yang, G., Hu, M., 2011. Acyl peroxy nitrate measurements during the photochemical smog season in Beijing, China. Atmos. Chem. Phys. Discuss. 2011, 10265–10303.
Xue, L., Wang, T., Wang, X., Blake, D.R., Gao, J., Nie, W., Gao, R., Gao, X., Xu, Z., Ding, A., Huang, Y., Lee, S., Chen, Y., Wang, S., Chai, F., Zhang, Q., Wang, W., 2014. On the use of an explicit chemical mechanism to dissect peroxy acetyl nitrate formation. Environ. Pollut. 195, 39–47.
Yang, W., Li, J., Wang, Z., Wang, L., Dao, X., Zhu, L., Pan, X., Li, Y., Sun, Y., Ma, S., Wang, W., Chen, X., Wu, J., 2020. Source apportionment of $PM_{2.5}$ in the most polluted Central Plains Economic Region in China: implications for joint prevention and control of atmospheric pollution. J. Clean. Prod. 283, 124557.
Ye, C., Chen, R., Chen, M., 2016. The impacts of Chinese Nian culture on air pollution. J. Clean. Prod. 112, 1740–1745.
Yuan, J., Ling, Z., Wang, Z., Lu, X., Fan, S., He, Z., Guo, H., Wang, X., Wang, N., 2018. PAN-precursor relationship and process analysis of PAN variations in the Pearl River Delta region. Atmosphere 9, 372.
Zeng, L., Fan, G.-J., Lyu, X., Guo, H., Wang, J.L., Yao, D., 2019. Atmospheric fate of peroxyacetyl nitrate in suburban Hong Kong and its impact on local ozone pollution. Environ. Pollut. 252, 1910–1919.
Zhang, J.M., Wang, T., Ding, A.J., Zhou, X.H., Xue, L.K., Poon, C.N., Wu, W.S., Gao, J., Zuo, H.C., Chen, J.M., Zhang, X.C., Fan, S.J., 2009. Continuous measurement of peroxyacetyl nitrate (PAN) in suburban and remote areas of western China. Atmos. Environ. 43, 228–237.
Zhang, J.B., Xu, Z., Yang, G., Wang, B., 2011. Peroxyacetyl nitrate (PAN) and peroxypropionyl nitrate (PPN) in urban and suburban atmospheres of Beijing, China. Atmos. Chem. Phys. Discuss. 11, 8173–8206.
Zhang, G., Mu, Y., Liu, J., Zhang, C., Zhang, Y., Zhang, Y., Zhang, H., 2014a. Seasonal and diurnal variations of atmospheric peroxyacetyl nitrate, peroxypropionyl nitrate, and carbon tetrachloride in Beijing. J. Environ. Sci. 26, 65–74.
Zhang, H., Xu, X., Lin, W., Wang, Y., 2014b. Wintertime peroxyacetyl nitrate (PAN) in the megacity Beijing: role of photochemical and meteorological processes. J. Environ. Sci. 26, 83–96.
Zhang, G., Mu, Y., Zhou, L., Zhang, C., Zhang, Y., Liu, J., Fang, S., Yao, B., 2015. Summertime distributions of peroxyacetyl nitrate (PAN) and peroxypropionyl nitrate (PPN) in Beijing: understanding the sources and major sink of PAN. Atmos. Environ. 103, 289–296.
Zhang, B., Zhao, B., Zuo, P., Huang, Z., Zhang, J., 2017. Ambient peroxyacetyl nitrate concentration and regional transportation in Beijing. Atmos. Environ. 166, 543–550.
Zhang, B., Zhao, X., Zhang, J., 2019. Characteristics of peroxyacetyl nitrate pollution during a 2015 winter haze episode in Beijing. Environ. Pollut. 244, 379–387.
Zhang, G., Xia, L., Zang, K., Xu, W., Zhang, F., Liang, L., Yao, B., Lin, W., Mu, Y., 2020. The abundance and inter-relationship of atmospheric peroxyacetyl nitrate (PAN), peroxypropionyl nitrate (PPN), O_3, and NO_y during the wintertime in Beijing, China. Sci. Total Environ. 718, 137388.
Zhao, S., Yin, D., Yu, Y., Kang, S., Qin, D., Dong, L., 2020. $PM_{2.5}$ and O_3 pollution during 2015–2019 over 367 Chinese cities: spatiotemporal variations, meteorological and topographical impacts. Environ. Pollut. 264, 114694.
Zhu, H., Gao, T., Zhang, J., 2018. Wintertime characteristic of peroxyacetyl nitrate in the Chengyu district of southwestern China. Environ. Sci. Pollut. Res. 25, 23143–23156.